Functionalized MCM-41 and CeMCM-41 Materials Synthesized via Interfacial Reactions

Valentyn Antochshuk,[†] Antonio S. Araujo,[‡] and Mietek Jaroniec*,[†]

Department of Chemistry, Kent State University, Kent, Ohio 44242, and Federal University of Rio Grande do Norte, Department of Chemistry, CP. 1662, 59078−970, Natal RN, Brazil

Received: June 16, 2000; In Final Form: August 9, 2000

A procedure of the template displacement by organosilanes was utilized to prepare pure-silica and cerium-substituted mesoporous materials with tailored surface functionality. These two self-assembled mesostructured systems exhibit hexagonal arrangement of mesopores but they show different reactivity with respect to organosilanes. Several samples with different pore size and functionality were prepared and for the first time a cerium-substituted mesostructured silicate was functionalized. Some peculiarities of organosilane interactions with the self-assembled cerium-substituted silicates reflect the difference in the acidic and coordination properties of cerium centers in the mesostructure. The study of the template displacement kinetics shows that about 4 h are needed to remove 70% of surfactant and about twice longer time is required for its complete removal. In addition, it is shown that the template displacement procedure stabilizes the ordered mesoporous structures.

Introduction

The discovery of nanoporous silicates with honeycomb arrangement of cylindrical (hexagonal) pores, such as MCM-41,[1] stimulated interest in the preparation of new three- and two-dimensional silica structures (FSM-16, MCM-48, SBA-15).[2] These materials, prepared through self-assembly of organic and inorganic precursors,[1] exhibit such unique properties as high surface area, large pore size and pore volume, pores accessible for large molecules.[3] A wide applicability of the aforementioned materials extended research interests beyond the silica and aluminosilicate materials. Recently, self-assembled materials such as metal sulfides,[4] metal oxides,[5] heterosubstituted silicates,[6] and inorganic−surfactant pairs[7] were discovered. Utilization of surfactants,[8] neutral amines,[9] and polymers[10] as structure-directing agents made possible to obtain materials with pore sizes up to 30 nm. Besides variations of the template size, the adjustment of pore sizes of mesoporous materials could be achieved by hydrothermal restructuring and synthesis under different temperature conditions.[11] Combining aforementioned synthetic procedures with possibilities of surface functionalization a wide variety of materials for chemical separations,[12] catalysis,[13] and environmental cleanup[14] could be obtained. Recently, novel organic−inorganic hybrid materials of uniformly distributed organic fragments in the entire inorganic framework were synthesized.[15] On the other hand, specific catalytic and adsorption applications require great selectivity of materials, which could be achieved by partial heterosubstitution of silica framework[16] and/or successful introduction of functional groups.[16a] Up to date lanthanide-substituted nanoporous materials were tried in many fields from catalysis to micro lasers[17] and one of the most frequently used lanthanides for catalytic applications is cerium.[18] Pure lanthanide oxides are not useful as catalysts (they are expensive and not very effective), but the promotional effect on oxide catalysts and prevention of the support sintering make them valuable additives in the applications such as automobile converters and catalytic wet oxidation of wastewater.[18] The recent synthesis[19] of lanthanide-incorporated mesoporous silicates showed an improvement in their thermal stability and structure properties such as the pore volume and surface area in comparison to pure MCM-41. Besides the framework changes due to introduction of heteroatoms, attachment of ligands to the pore walls is another method to modify the surface chemistry of inorganic materials. Such manipulations can significantly change hydrophilic−hydrophobic properties as well as introduce organic groups on the surface.

It was recently shown[20,21] that the template displacement with organosilanes is an attractive method to obtain the surfactant-free mesoporous silicates and simultaneously alter their surface functionality. Unlike conventional calcination[1] or one-pot synthesis,[22] this procedure does not require high temperature calcination step and/or surfactant extraction. The additional advantages of this displacement procedure are simultaneous introduction of chemical functionality, the possibility of recovering surfactant, and stabilization of the samples, which partially or completely disintegrate upon temperature treatment. A general idea of this displacement process is based on the reaction of uncalcined self-assembled mesoporous materials containing structure-directing surfactant inside of prospective mesopores with organosilanes.[21] The variation in the functionality of silane molecules creates possibility to alter the pore size and pore chemistry of the resulting mesoporous materials.

The current work presents a systematic study of the template displacement procedure with organosilanes (TDS) for the pure MCM-41 and cerium-substituted mesoporous silicates. A comparison of this process for two different mesostructured silicates showed some similarities but also some differences in interactions of silanes with the self-assembled pure and cerium-substituted silicates. Namely, the template displacement procedure provides not only the surface functionalized materials but also preserves structure and stabilizes their ordered framework, which often collapses upon temperature treatment. The study of the reaction kinetics of silane with silicates showed

* To whom correspondence should be addressed. Fax: (330) 672-3816. E-mail: jaroniec@columbo.kent.edu.
[†] Department of Chemistry.
[‡] Federal University of Rio Grande do Norte.

10.1021/jp0021648 CCC: $19.00
Published on Web 09/20/2000

that the displacement process requires reaction time about 4 h for 70% surfactant removal and twice more time for a complete surfactant removal.

Methods and Materials

Materials. Fumed silica M-5 (Cab-O-Sil) from Cabot Co. (Tuscola, IL) and cerium (III) chloride heptahydrate, sodium hydroxide, cetyltrimethylammonium bromide (CTMAB) from Aldrich Chemical Co. (Milwaukee, WI) were used in preparation of mesoporous silicates. Hexane and *iso*-propanol solvents (HPLC grade, water content below 0.02%) were from Fisher Scientific (Pittsburgh, PA) and toluene (water content below 0.001%) was from Aldrich Chemical Co. (Milwaukee, WI). The (3-cyanopropyl)dimethylchlorosilane, (3-amino-propyl)triethoxysilane, *n*-octyldimethylchlorosilane, and *n*-octyltriethoxysilane were from Aldrich Chemical Co. (Milwaukee, WI). All materials were used without additional purification.

Synthesis. The pure siliceous and cerium-substituted MCM-41 materials were prepared using the same molar gel composition: $4SiO_2$:1 Na_2O:1CTMAB:200H_2O. For preparation of the Ce-substituted MCM-41 material, the appropriate amount of cerium chloride was added to obtain the Si/Ce ratio equal to 1:50. The preparation procedure used included dissolution of silica in 1 M sodium hydroxide solution at 70 °C followed by addition of surfactant solution (CTMAB). The obtained mixture was stirred for about 1 h to obtain a homogeneous gel. For the Ce-substituted MCM-41 material, $CeCl_3 \cdot 7H_2O$ was added to the gel and aged for additional 1 h. Both gels were treated under autogenous pressure at 100 °C for 4 days by adjusting pH to about 10 followed by salt addition. The resulting samples were filtered and washed with deionized water, and finally dried at 100 °C. Two samples were prepared: pure-silica and Ce-substituted MCM-41, designated as Si−U and Ce−U, respectively. Typical amount of the prepared sample was around 4 g. The Si−U and Ce−U samples calcined at 550 °C, 2 h in nitrogen and 4 h in dry air atmosphere, heating rate 2.5 °C min^{-1}, were designated as Si−C and Ce−C, respectively.

The one-step procedure for preparation of mesoporous silicates with simultaneous surfactant removal was carried out to obtain functionalized samples. All functionalized materials were prepared by reaction of the appropriate silane with the uncalcined MCM-41 material without its initial pretreatment as it was previously described.[20,21] In a typical procedure, 12 mL of silane was added to about 0.25 g of "as-synthesized" silica-surfactant material and mixture was refluxed for 4−15 h. The silanes used reacted with silanols and successfully displaced the surfactant contained inside of the self-assembled structure. The resulting white solid was filtered, washed with benzene and *i*-propanol, and dried under vacuum for 6 h at 90 °C. All samples showed any change in color, but samples modified with octylsylil groups were of light-gray color. The pure-silica samples obtained in the one-step procedure with octyldimethylchlorosilane and cyanopropyldimethylchlorosilane, and (aminopropyl)triethoxysilane were designated as Si−UO, Si−UCN, and Si−UENH_2, correspondingly. To investigate the kinetics of modification process the synthesis with octyltriethoxysilane was performed for different reaction times (4 and 6 h) and the resulting samples were designated Si−UEO 4 h and Si−UEO 6h, correspondingly. The cerium-substituted materials obtained in the one-step procedure with octyldimethylchlorosilane, octyltriethoxysilane and (aminopropyl)triethoxysilane were designated as Ce−UO, Ce−UEO, and Ce−UENH_2, correspondingly.

Characterization Methods. X-ray powder diffraction data were collected on a Siemens D5005 diffractometer using Cu Kα radiation ($\lambda = 0.154056$ nm) within the 2θ range of 1.5−10°. The interplanar spacing (XRD d_{100}, nm) was calculated from the position of the first low-angle peak.

Nitrogen adsorption measurements were carried out using a Micromeritics model ASAP 2010 adsorption analyzer (Norcross, GA). Adsorption isotherms were measured at −196 °C over the interval of relative pressures from 10^{-6} to 0.995 using nitrogen of 99.998% purity. Before analysis each sample was degassed for 2 h at 120 °C under vacuum of about 10^{-3} Torr in the degas port of the adsorption apparatus. Adsorption data in the range of relative pressures $p/p_0 = 0.04-0.14$ were used to calculate the BET specific surface area (S_{BET}, $m^2\ g^{-1}$) of the materials studied.[23] Pore size distributions were calculated from adsorption branches of nitrogen isotherms using the BJH method with corrected form of the Kelvin equation for capillary condensation in cylindrical pores.[24] The position of the peak maximum is referred as the pore width (w_{pore}, nm).

^{13}C and ^{29}Si CP-MAS and ^{29}Si single-pulse MAS NMR experiments[25] were performed on a Bruker NMR spectrometer model Avanchi 400DMX NMR (Bruker Instrument, Inc., San Jose, CA) operating at resonance frequencies of 100.54 and 79.49 MHz for ^{13}C and ^{29}Si, respectively. Measurements were performed at a room temperature, air was used as driving and bearing gas. Material was spun in a 7 mm zirconia rotor at the magic angle with the spinning frequency of 2.5 kHz. The total number of scans in the ^{13}C CP-MAS, ^{29}Si CP-MAS, and ^{29}Si single-pulse experiments were 10000, 2000, and 800, correspondingly. ^{13}C spectra were acquired with 1 ms contact time and a recycle time 5 s. ^{29}Si CP-MAS spectra were obtained with 10 ms contact time and a recycle time 2 s. A high-power decoupling was used during acquisition. During ^{29}Si single-pulse experiment with inverse gated decoupling, the repetition delays of 180−300 s, taken as $5T_1$ for slowest relaxing site, were used. Considering long spin−lattice relaxation time of low abundant ^{29}Si nucleus, the relaxation times T_1 of all silicon sites were preliminary estimated with a saturation recovery procedure. Chemical shifts were externally referenced to liquid tetramethylsilane (TMS). All chemical shifts are reported in parts per million.

The content of carbon, nitrogen, and hydrogen in the samples was determined using a LECO model CHNS-932 elemental analyzer (St. Joseph, MI). The BET specific surface area as well as carbon and hydrogen contents from elemental analysis were used to estimate the concentrations of attached ligands. Their concentrations were related to 1 g of unmodified material (C_{lig}, mmol g^{-1}).

TA Instruments model TA 2950 (New Castle, DE) analyzer was used to carry out high-resolution thermogravimetric analysis (nitrogen atmosphere, temperature range from 25 to 1000 °C, heating rate 5 °C min^{-1}).

Results and Discussion

Synthesis of pure-silica and cerium-incorporated self-assembled surfactant−silicate systems was accomplished in accordance with typical procedure that included the pH adjustment and salt addition.[26] In the final stage of preparation, each sample was split on two parts. The first part, for comparison purposes, was subjected to calcination. The second part of the freshly prepared sample was subjected to the template displacement synthesis (TDS).[21]

The resulting calcined materials (Table 1) had large surface areas and pore volumes that together with characteristic XRD spectra (Figure 1A) and condensation step on the nitrogen adsorption isotherms (Figure 2A) prove their mesoporosity.

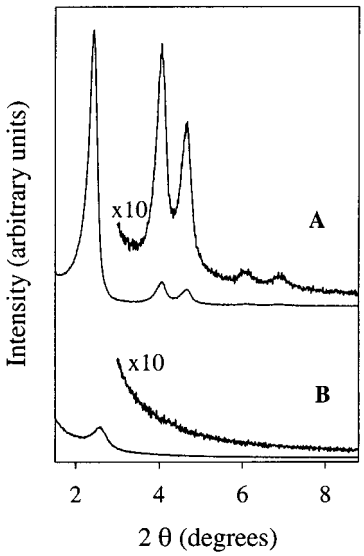

Figure 1. X-ray powder diffraction patterns for the calcined materials studied: (A) pure-silica (B) and collapsed cerium-substituted material. Inserts show enlarged area of the 110, 200, 210, and 300 peaks.

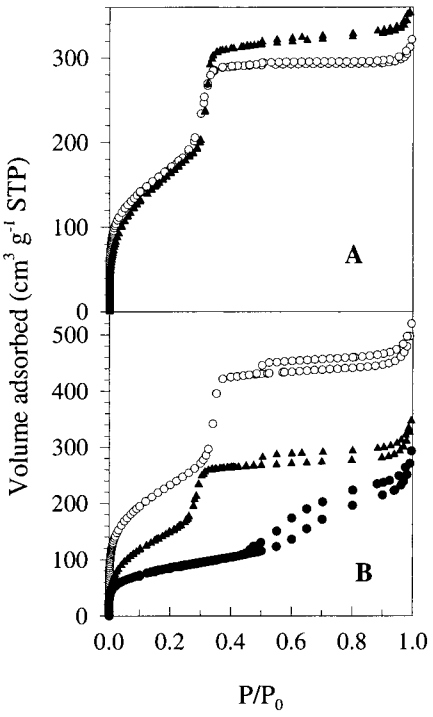

Figure 2. Nitrogen adsorption isotherms for the (A) Si−MCM and (B) Ce−MCM samples. Open circles refer to the samples after calcination and the closed triangles refer to the samples prepared by the TDS process with (aminopropyl)triethoxysilane. For comparison, the isotherm for the collapsed Ce-substituted calcined sample is shown (closed circles).

Adsorption studies of the pure-silica and cerium-substituted MCM-41 samples showed an increase in the surface area and pore volume by about 40% for the sample with cerium in the framework prepared under similar conditions (BET surface area 605 and 845 $m^2\ g^{-1}$, BJH pore volume 0.5 and 0.8 $cm^3\ g^{-1}$, for pure-silica and cerium-substituted samples, correspondingly). A slightly higher adsorption in the low-pressure region, observed for the cerium-substituted MCM-41, provides an evidence for lower hydrophobicity, which was caused by incorporation of cerium heteroatoms into the structure. The preliminary studies suggest that the incorporation of cerium into the framework of mesoporous silicates caused, besides an increase in the pore volume and surface area, an improvement in their thermal and hydrothermal stability as well.[19] However, the long-term stability of calcined samples requires further studies. It was noted that upon seven month of storage, a good quality freshly calcined cerium-substituted mesosilicate, with a sharp condensation step on the nitrogen adsorption isotherm (see Figure 2B), was disintegrated. The disintegration of calcined cerium-incorporated material is also evident from the XRD data (Figure 1B), whereas the surface area and pore volume of the pure MCM-41 sample, synthesized under similar conditions, was not changed with time. While some gain in the short-term stability and structural parameters of the Ce-substituted sample is obvious, the presence of heteroatoms in the MCM-41 may reduce the sample hydrophobicity, and consequently, may alter the long-term properties of the samples. Despite the observed long-term instability of the cerium-substituted MCM-41 sample studied, this material could be stabilized via recently proposed template displacement synthesis (TDS).[20]

The TDS procedure takes advantage of the high stability of "as-prepared" self-assembled systems, which in fact are stable over a long time. The inherent instability of some calcined samples, caused by the exposure of strained siloxane bonds to environment, is avoided in the synthesis of MCM-41 materials via TDS procedure. The preparation of mesoporous silicates through interfacial reaction (direct displacement of the templating surfactant in the uncalcined self-assembled material) provides the materials with functionalized surface and pore sizes in the range of 2−4 nm (Table 1). The TDS procedure allows one to tailor the pore diameter by introduction groups of desired sizes. Moreover, the surface properties, such as hydrophobicity and chelating capability, can be adjusted by choosing organosilanes of required structure and functionality. Almost any silane

TABLE 1: Structural Parameters of the Self-assembled Materials Studied

sample	mesopore volume ($cm^3\ g^{-1}$)	surface area S_{BET} ($m^2\ g^{-1}$)	XRD spacing d_{100} (nm)	pore width w_{pore} (nm)	ligand-loading C_{lig} (mmol g^{-1} SiO_2)
Si−U		*a*	4.09		
Si−C	0.50	605	3.63	3.55	
Si−UENH$_2$	0.57	600	3.96	3.40	1.4
Si−UEO 4h	0.49	670	3.98	2.85	1.1
Si−UEO 6h	0.38	500	4.05	2.65	1.8
Si−UO	0.31	405		2.40	2.4
Si−UCN	0.38	415	4.05	3.00	2.5
Ce−U		*a*	3.80		
Ce−C	0.80	845		3.75	
Ce−UO	0.31	385	3.94	2.40	2.3
Ce−UEO	0.40	480	3.91	2.60	1.9
Ce−UENH$_2$	0.54	545	3.96	3.20	1.5

[a] Surface area was in the order of several $m^2\ g^{-1}$.

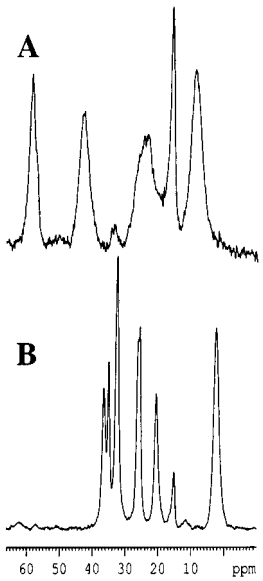

Figure 3. ^{13}C CP-MAS spectra for the mesoporous materials prepared via interfacial reaction with (A) (aminopropyl)triethoxysilane and (B) octyldimethylchlorosilane. Signals in the ^{13}C NMR spectrum of the treated samples are characteristic for attached silane molecules and the position of peaks corresponds to the ones that can be found in the case of pure silanes.

that has at least one "reactive group" (either Cl− or Et(Me)O−) could displace template from self-assembled mesostructured systems.[21] The expulsion of surfactant from the self-assembled mesostructure and subsequent attachment of functional groups were proved by means of ^{13}C and ^{29}Si NMR, nitrogen adsorption, elemental analysis, and high-resolution thermogravimetry.

The uncalcined "as-prepared" mesostructured material exhibits several peaks on the ^{13}C NMR spectra (chemical shifts from 15 to 70 ppm) resembling the data for cetyltrimethylammonium bromide solution but with broader peaks that are characteristic for the solid-state NMR (spectra are not shown). The observed minor change in the peaks for carbon atoms close to the headgroup (namely, methyl groups of the headgroup and the first and second methylenes counting from the trimethylammonium headgroup) indicates that the surfactant headgroup is electrostatically attached to silicate.[27] A transformation of the surfactant-silica mesostructured assemblies upon interfacial reaction with silanes is evidenced by changes in the ^{13}C CP-MAS solid-state NMR spectra. There are several signals in the ^{13}C NMR spectrum of the treated sample characteristic for attached silane molecules (Figure 3). The position of peaks resembles ones that can be found for pure silanes. The presence of peaks at 16 and 58 ppm for the sample prepared with triethoxysilane (Figure 3A) proves that not all ethoxy groups are hydrolyzed under conditions of the template displacement synthesis, which was additionally confirmed by the CHN analysis.

The ^{29}Si NMR spectra of the template-displaced silica exhibit several typical signals that originate from the silicon atoms in various chemical environments, such as siloxane [(≡Si−O−)$_4$Si*] Q_4 at −110 ppm, single silanol [(≡Si−O−)$_3$Si*−OH] Q_3 at −100 ppm. Upon introduction of silane, additional signal(s) from the silicon atom of attached ligands appear. The attachment of alkylmonochlorosilane [(≡Si−O−)Si*(R)R′$_2$] results in the single peak at ca. 15 ppm because there is only one reactive group in silane molecule and only one possible structure could be formed upon this attachment. Interactions with trialkoxysilane could give rise up to three

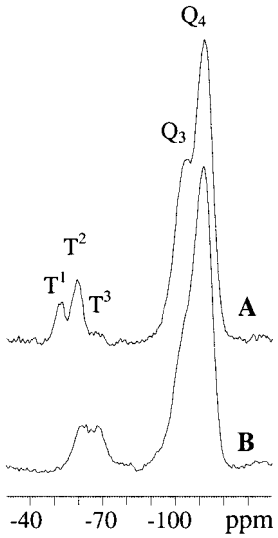

Figure 4. ^{29}Si CP-MAS spectra for the mesoporous materials prepared via TDS process with (A) octyltriethoxysilane for 6 h and (B) (aminopropyl)triethoxysilane. See text for description.

different signals depending on the way of attachment. When the interaction of silane molecule lead to the formation of only one bond with surface [(≡Si−O−)Si*(OR′$_2$)R], only one signal at −50 ppm and an island structure T^1 is visible. The formation of two bonds with the silica surface [(≡Si−O−)$_2$Si*(OR′)R] or a terminal attachment (silane interacts in a monomeric fashion with surface and simultaneously forms one bond with neighboring attached silane) would give rise to signal at −58 ppm (T^2 structure). The signal arising from the silane bonded in a tridentate fashion with the silica surface [(≡Si−O−)$_3$Si*R] or the silane that form cross-links on the surface (cross-link with neighboring attached silanes) would give peak at −68 ppm (T^3-type attachment).

When trialkoxysilanes were utilized in the TDS procedure, the amount of different structural types (T^1, T^2, or T^3) varied significantly, depending on the silane used (Figure 4). The displacement of surfactant from the mesostructure with triethoxyoctylsilane resulted in all T^1, T^2, and T^3 type structures present in the sample (Figure 4A). On the other hand, reaction with triethoxyaminopropylsilane gave sample with only T^2 and T^3 structures available (Figure 4B). The aforementioned difference in the spectra and lower surface coverage of relatively small aminopropylsilyl ligands could be rationalized by assuming that aminopropylsilane interacts with the silica surface mostly in bi- and tridentate fashion (T^2 and T^3 structures) forming two and three Si−O−Si attachments to the surface and there is no significant cross-linking between neighboring silanes. For the samples prepared with monochlorosilanes only the signal at 15 ppm arising from the silane attached in a monomeric fashion was observed (spectrum is not shown).

The single-pulse ^{29}Si NMR spectra, which are equally sensitive to both Q_3 and Q_4 signals, indicate that after surfactant displacement and silane attachment the amount of free silanols is reduced (Figure 5). An increase in the amount of attached functionality results in the higher intensity of signal at −110 ppm and smaller intensity of the signal at −100 ppm. The amount of bonded silyl groups, evaluated from the deconvolution of the Q_3 and Q_4 signals of NMR data, was very close to that found by elemental analysis.

A significantly reduced low-pressure nitrogen adsorption for the samples prepared by TDS procedure in comparison to the corresponding calcined samples confirms the attachment of

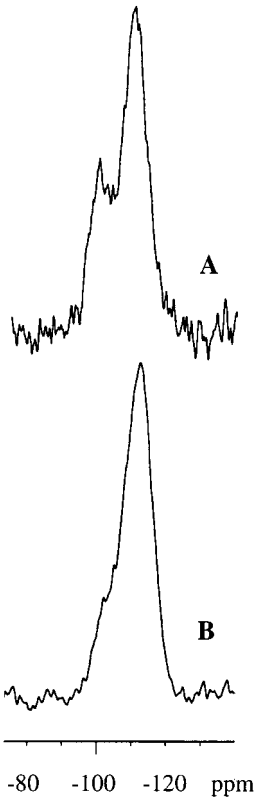

Figure 5. ^{29}Si single-pulse MAS spectra for the (A) uncalcined mesostructured sample and the (B) material prepared via interfacial reaction with (aminopropyl)triethoxysilane.

hydrophobic groups to the silica surface (data not shown). The sequence of low-pressure nitrogen isotherms for the MCM-41 samples prepared by TDS procedure allowed us to order the samples with decreasing hydrophobicity: MCM-41 with octyl-groups > MCM-41 with cyanopropyl-groups > MCM-41 with aminopropyl-groups > calcined MCM-41 samples. Nitrogen adsorption isotherms (Figure 2) measured for the samples prepared with organosilanes showed smaller pore volume than the corresponding calcined samples due to the ligand attachment. However, a comparison of adsorption data for calcined pure-silica and cerium-substituted MCM-41 samples and those prepared with aminopropylsilane revealed that the materials with and without heterosubstitution behave differently upon functionalization. If the Ce−UENH$_2$ material showed significant drop in the amount adsorbed in comparison to the Ce−C sample, the Si−UENH$_2$ and Si−C samples differed only slightly (Figure 2). If one takes into account that the Si−UENH$_2$ sample had the loading of grafted groups of 1.4 mmol g^{-1}, such a small difference in the surface area, pore size, and pore volume of Si−UENH$_2$ and Si−C (Table 1) is surprising.

The surface coverages of attached ligands for the samples prepared via reaction with organosilanes, found by the CHN analysis, were in the range 1.4−2.5 mmol g^{-1}. The elemental analysis results suggest that the samples prepared with alkoxysilanes have ligands attached in a monomeric fashion and the side RO-groups are not hydrolyzed. Such attachment makes difficult to obtain higher bonding coverage. In contrast, higher ligand loadings were achieved for chlorosilanes (Table 1). Our studies indicate that the displacement of templating surfactant is not always complete. So, the calculation of the surface coverage was carefully performed by comparing, whenever it was possible, with the results from carbon and nitrogen analysis to take into account the residual amounts of the template. The

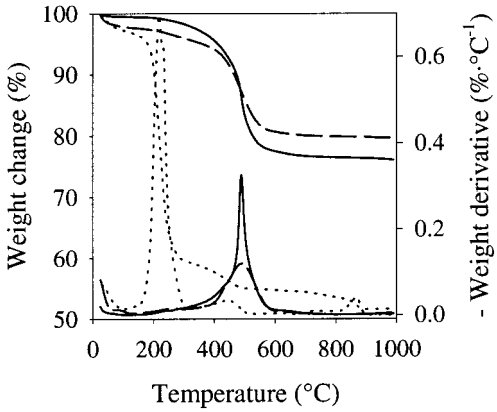

Figure 6. TG and DTG curves for the (dotted lines) uncalcined pure MCM-41 and the samples prepared by the TDS process with octyltriethoxysilane during (dashed lines) 4 h and (solid lines) 6 h.

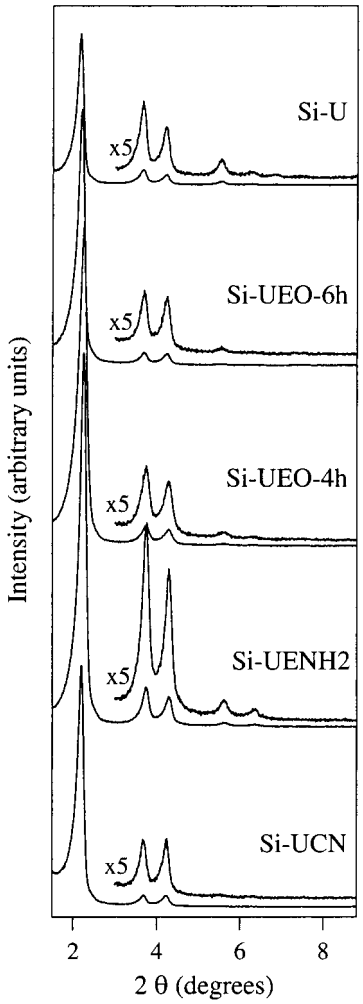

Figure 7. X-ray powder diffraction patterns for the uncalcined pure MCM-41 and the materials prepared by template displacement reaction with the following silanes: octyltriethoxysilane, (aminopropyl)triethoxysilane and cyanopropyldimethylchlorosilane. Inserts show enlarged area of the 110, 200, 210, and 300 peaks.

typical surfactant residue for the samples prepared with alkoxysilanes was 0.5−1% (for cerium-substituted samples up to 6%) of the initial amount of surfactant. For both pure-silica and cerium-substituted samples prepared with chlorosilanes the surfactant residue was higher, 6% and 10%, correspondingly. The effectiveness of the surfactant displacement could be some indication of the pore accessibility (presence of void spaces

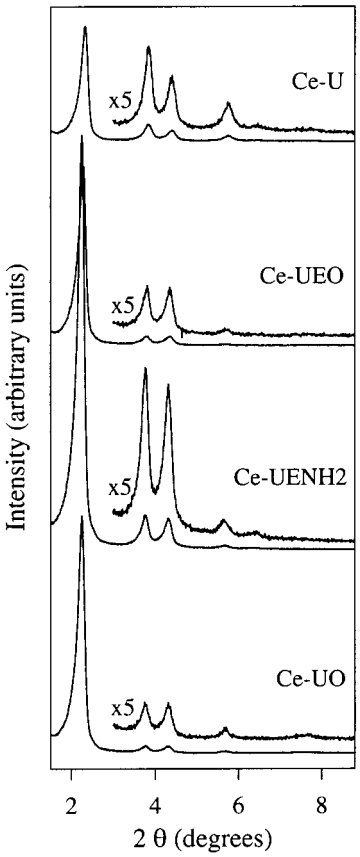

Figure 8. X-ray powder diffraction patterns for the cerium-incorporated mesostructured materials: uncalcined, and the materials prepared by TDS with the following silanes: octyltriethoxysilane, (aminopropyl)-triethoxysilane, and octyldimethylchlorosilane. Inserts show enlarged area of the 110, 200, 210, and 300 peaks.

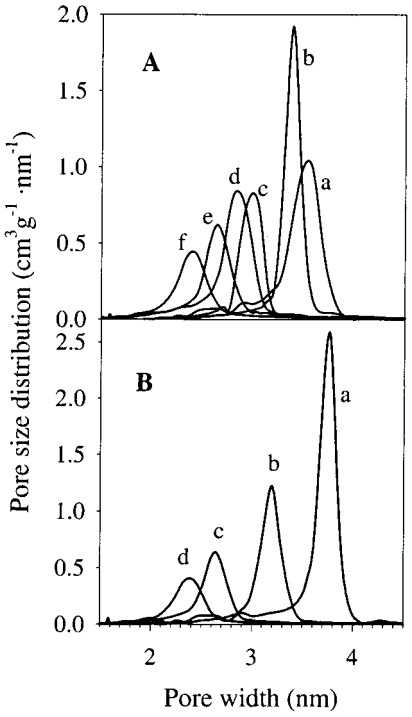

Figure 9. Differential pore size distributions calculated from the nitrogen adsorption isotherms for the Si−MCM-41 sample (part A): (a) after calcination, (b) after the TDS process involving (aminopropyl)-triethoxysilane, (c), cyanopropyldimethylchlorosilane, (d and e) octyl-triethoxysilane, (f) and octyldimethylchlorosilane. The Ce−MCM samples (part B): (a) after calcination, (b) after TDS process involving (aminopropyl)triethoxysilane, (c) octyltriethoxysilane, and (d) octyldi-methylchlorosilane.

unaccessible for silanes) and surface acidity (which is higher in the case for the cerium-incorporated sample). Because the TDS process is usually performed at relatively low temperatures (∼100−150 °C), it should occur without surfactant decomposition that may allows one to recover the template.

In accordance with thermogravimetric analysis (Figure 6), the process of surfactant displacement from as-synthesized mesostructured materials with silanes is quite fast, and proceeds during only several hours. Even 4 h exposure of an uncalcined sample to silane is sufficient to remove surfactant from the pores and to achieve about 60% of the maximum ligand density. A distinctly higher (ca. 2%) weight change at temperatures around 100 °C for the Si−UEO 4 h in comparison to the Si−UEO 6 h sample (see Figure 6) once again shows that the silica surface is partially opened and is readily accessible for water molecule adsorption. A dense layer of octyl ligands in the Si−UEO 6 h sample makes the pore walls highly hydrophobic and reduces the water adsorption. An almost complete removal of the surfactant template by alkoxysilanes is evident on the DTG curves by disappearance of the peak at ca. 230 °C and appearance of new one at ca. 500 °C, which correspond to the decomposition of CTAB surfactant and attached octyldiethoxy-silyl groups, correspondingly. As it was mentioned above, for the samples prepared with alkoxysilanes, the surfactant residue was negligible (equal or less than 1%).

The XRD data of the materials prepared via TDS procedure (Figures 7 and 8) revealed that the structure of mesoporous framework is preserved during the process of a simultaneous template displacement and functionalization. All samples showed four or five peaks in their XRD spectra. Also, in the case of the Si−$UENH_2$ and Ce−$UENH_2$ samples, a higher intensity of peaks in comparison to those for the corresponding calcined samples suggests that the structural ordering has been improved. The XRD (100) interplanar spacing for the pure-silica amino-propyl functionalized material was similar to the uncalcined sample and about 0.3 nm larger than that for the calcined one. For the cerium-substituted aminopropyl functionalized MCM-41 sample, the d_{100}-spacing was about 0.15 nm larger than that for the corresponding uncalcined sample. This was achieved partially by avoiding calcination, which otherwise causes shrinkage of the sample.

Calculations of the pore size distributions (Figure 9 and Table 1) showed the pore opening upon TDS procedure. As it could be expected, the introduction of functional groups into the mesopores resulted in most cases in a decrease of the width and volume of mesopores that is common for a conventional modification procedure. A significant deviation from this trend was observed upon application of aminosilanes in the TDS procedure. The pure-silica MCM-41, treated with (aminopropyl)-triethoxysilane showed a large pore volume (almost 0.1 cm^3 g^{-1} larger) and very similar pore size (only 0.15 nm smaller) than the corresponding pure-silica calcined material. It also should be mentioned that the TDS procedure significantly improves the pore ordering of the pure-silica MCM-41 sample with aminopropyl groups (Si−$UENH_2$), which is manifested by narrowing the pore size distribution in comparison to the calcined material (Si−C) (Figure 9A). A similar trend is visible from the XRD data. It appears that aminopropyl-triethoxysilane acts not only as expelling reagent and surface modifier but also it slightly expands the mesoporous structure. This expansion process may be analogous to the hydrothermal restructuring of uncalcined self-assembled silicates[28] in the presence of amines.[11b]

The avoiding of shrinkage (by eliminating of calcination step) and some expansion of the mesostructure upon treatment aminopropylsilane is an attractive feature, which requires further studies.

The aforementioned synthesis of the cerium-substituted MCM-41 via surfactant displacement procedure allowed us to obtain the mesoporous silicates with functionalized surface otherwise these materials may disintegrate upon calcination. Thus, the functionalization of the metal-incorporated mesoporous silicates is of great importance not only for increasing their hydrothermal stability but also for tailoring their catalytic functionality. Even though the TDS procedure affords only materials with functionalized surfaces, in contrast to the calcination that gives bare-silica surfaces, the flexibility in the selection of grafted groups and ability to stabilize the mesopore structure of the samples, which may disintegrate, makes this procedure worthy to explore for preparation of new materials.

Conclusions

It was shown that a simultaneous pore opening and surface functionalization of the cerium-substituted and pure-silica MCM-41 materials could be done easily by a direct displacement of the templating surfactant with suitable organosilanes. Although there is a clear advantage in the obtaining high surface area and large pore materials via introduction of a small amounts of cerium into the mesostructure, a long-term stability of hetero-substituted MCM-41 must be carefully inspected. A current study shows the results of the stabilization and improvement of the MCM-41 structures by a direct functionalization of self-assembled mesostructured systems with organosilanes. The utilized procedure allows one to prepare the mesoporous silicates without high-temperature calcination (which can cause some disintegration of ordered structures), by avoiding the pore shrinkage and making the template regeneration possible.

Acknowledgment. The authors thank Dr. SongPing Huang and Mr. Chibiao Liu (Kent State University) for XRD measurements. The donors of the Petroleum Research Fund administrated by the American Chemical Society are gratefully acknowledged for partial support of this research.

References and Notes

(1) (a) Kresge, C. T.; Leonowicz, M. E.; Roth, W. J.; Vartuli, J. C.; Beck, J. S. *Nature* **1992**, *359*, 710−712. (b) Beck, J. S.; Vartuli, J. C.; Roth, W. J.; Leonowicz, M. E.; Kresge, C. T.; Schmitt, K. D.; Chu, C. T.-W.; Olson, D. H.; Sheppard, E. W.; McCullen, S. B.; Higgins J. B.; Schlenker, J. L. *J. Am. Chem. Soc.* **1992**, *114*, 10834−10843.

(2) (a) Inagaki, S.; Fukushima, Y.; Kuroda, K. *J. Chem. Soc., Chem. Commun.* **1993**, 680−681. (b) Vartuli, J. C.; Schmitt, K. D.; Kresge, C. T.; Roth, W. J.; Leonowicz, M. E.; McCullen, S. B.; Hellring, S. D.; Beck, J. S.; Schlenker, J. L.; Olson, D. H.; Sheppard, E. W. *Chem. Mater.* **1994**, *6*, 2317−2326. (c) Zhao, D. Y.; Feng, J. L.; Huo, Q. S.; Melosh, N.; Fredrickson, G. H.; Chmelka, B. F.; Stucky, G. D. *Science* **1998**, *279*, 548−552.

(3) (a) Luan, Z.; Xu, J.; Kevan, L. *Chem. Mater.* **1998**, *10*, 3699−3706. (b) O'Brien, S.; Keates, J. M.; Barlow, S.; Drewitt, M. J.; Payne, B. R.; O'Hare, D. *Chem. Mater.* **1998**, *10*, 4088−4099.

(4) (a) Li, J.; Kessler, H.; Delmotte, L. *J. Chem. Soc., Faraday Trans.* **1997**, *93*, 665−668. (b) Neeraj, Rao, C. N. R. *J. Mater. Chem.* **1998**, *8*, 279−280.

(5) Huo, Q. S.; Margolese, D. I.; Ciesla, U.; Feng, P. Y.; Gier, T. E.; Sieger, P.; Leon, R.; Petroff, P. M.; Schuth, F.; Stucky. G. D. *Nature* **1994**, *368*, 317−321.

(6) (a) Zhang, W. H.; Froba, M.; Wang, J. L.; Tanev, P. T.; Wong, J.; Pinnavaia, T. J. *J. Am. Chem. Soc.* **1996**, *118*, 9164−9171. (b) Kosslick, H.; Landmesser, H.; Fricke, R. *J. Chem. Soc., Faraday Trans.* **1997**, *93*, 1849−1854. (c) Kruk, M.; Jaroniec, M.; Sayari, A. *Langmuir* **1999**, *15*, 5683−5688.

(7) Ying, J. Y.; Mehnert, C. P.; Wong, M. S. *Angew. Chem., Int. Ed. Engl.* **1999**, *38*, 56−77.

(8) Huo, Q.; Margolese, D. I.; Ciesla, U.; Demuth, D. G.; Feng, P.; Gier, T. E.; Sieger, P.; Firouzi, A.; Chmelka, B. F.; Schuth, F.; Stucky. G. D. *Chem. Mater.* **1994**, *6*, 1176−1191.

(9) Tanev, P. T.; Pinnavaia, T. J. *Science* **1995**, *267*, 865−867.

(10) (a) Bagshaw, S. A.; Prouzet, E.; Pinnavaia, T. J. *Science* **1995**, *269*, 1242−1244. (b) Zhao, D.; Huo, Q.; Feng, J.; Chmelka, B. F.; Stucky, G. D. *J. Am. Chem. Soc.* **1998**, *120*, 6024−6036.

(11) (a) Huo, Q.; Margolese, D. I.; Stucky, G. D. *Chem. Mater.* **1996**, *8*, 1147−1160. (b) Kruk, M.; Jaroniec, M.; Sayari, A. *J. Phys. Chem. B* **1999**, *103*, 4590−4598. (c) Kruk, M.; Jaroniec, M.; Sakamoto, Y.; Terasaki, O.; Ryoo, R.; Ko, C. H. *J. Phys. Chem. B* **2000**, *104*, 292−301.

(12) Thoelen, C.; Van de Walle, K.; Vankelecom, I. F. J.; Jacobs, P. A. *Chem. Commun.* **1999**, 1841−1842.

(13) (a) Maschmeyer, T.; Rey, F.; Sankar, G.; Thomas, J. M. *Nature* **1995**, *378*, 159−162. (b) Sayari, A. *Chem. Mater.* **1996**, *8*, 1840−1852. (c) Mehnert, C. P.; Weaver, D. W.; Ying, J. Y. *J. Am. Chem. Soc.* **1998**, *120*, 12289−12296.

(14) (a) Feng, X.; Fryxell, G. E.; Wang, L.-Q.; Kim, A. Y.; Liu, J.; Kemner, K. M. *Science* **1997**, *276*, 923−926. (b) Liu, J.; Feng, X.; Fryxell, G. E.; Wang, L.-Q.; Kim, A. Y.; Gong, M. *Adv. Mater.* **1998**, *10*, 161−165. (c) Mercier, L.; Pinnavaia, T. J. *Environ. Sci. Technol.* **1998**, *32*, 2749−2754. (d) Macquarrie, D. J. *Green Chem.* **1999**, *1*, 195−198.

(15) (a) Inagaki, S.; Guan, S.; Fukushima, Y.; Ohsuna, T.; Terasaki, O. *J. Am. Chem. Soc.* **1999**, *121*, 9611−9614. (b) Melde, B. J.; Holland, B. T.; Blanford, C. F.; Stein, A. *Chem. Mater.* **1999**, *11*, 3302−3308. (c) Asefa, T.; MacLachlan, M. J.; Coombs, N.; Ozin, G. A. *Nature* **1999**, *402*, 867−871.

(16) (a) Corma, A. *Chem. Rev.* **1997**, *97*, 2373−2419. (b) Klein, S.; Martens, J. A.; Parton, R.; Vercruysse, K.; Jacobs, P. A.; Maier, W. F. *Catal. Lett.* **1996**, *38*, 209−214. (c) Armengol, E.; Corma, A.; Garcia, H.; Primo, J. *Eur. J. Org. Chem.* **1999**, *1915*, 5−1920.

(17) Yang, P. D.; Wirnsberger, G.; Huang, H. C.; Cordero, S. R.; McGehee, M. D.; Scott, B.; Deng, T.; Whitesides, G. M.; Chmelka, B. F.; Buratto, S. K.; Stucky, G. D. *Science* **2000**, *287*, 465−467.

(18) Trovarelli, A.; de Leitenburg, C.; Boaro, M.; Dolcetti, G. *Catal. Today* **1999**, *50*, 353−367.

(19) (a) He, N. H.; Bao, S. L.; Xu, Q. H. *Stud. Surf. Sci. Catal.* **1997**, *105*, 85−92. (b) Zhang, W.; Pinnavaia, T. J. *Chem. Commun.* **1998**, 1185−1186. (c) Araujo, A. S.; Jaroniec, M. *J. Coll. Interface Sci.* **1999**, *218*, 462−467. (d) Araujo, A. S.; Jaroniec, M. *Stud. Surf. Sci. Catal.* **2000**, *129*, 187−194.

(20) Antochshuk, V.; Jaroniec, M. *Chem. Commun.* **1999**, 2373−2374.

(21) Antochshuk, V.; Jaroniec, M. *Chem. Mater.* **2000**, *12*, 2496−2501.

(22) (a) Burkett, S. L.; Sims, S. D.; Mann, S. *J. Chem. Soc., Chem. Commun.* **1996**, 1367−1368. (b) Lim, M. H.; Blanford, C. F.; Stein, A. *J. Am. Chem. Soc.* **1997**, *119*, 4090−4091.

(23) (a) Brunauer, S.; Emmett, P. H.; Teller, E. *J. Am. Chem. Soc.* **1938**, *60*, 309−319. (b) Roquerol, J.; Avnir, D.; Fairbridge, C. W.; Everett, D. H.; Hayness, J. H.; Pernicone, N.; Ramsay, J. D. F.; Sing, K. S. W.; Unger, K. K. *Pure Appl. Chem.* **1994**, *66*, 1739−1758.

(24) Kruk, M.; Jaroniec, M.; Sayari, A. *Langmuir* **1997**, *13*, 6267−6273.

(25) Harris, R. K.; Mann, B. E. *NMR and the Periodic Table*; Academic Press: London, 1978.

(26) Ryoo, R.; Jun, S. *J. Phys. Chem. B* **1997**, *101*, 317−320.

(27) Wang, L.-Q.; Exarhos, G. J.; Liu, J. *Adv. Mater.* **1999**, *11*, 1331−1341.

(28) Khushalani, D.; Kuperman, A.; Ozin, G. A.; Tanaka, K.; Garces, J.; Olken, M. N.; Coombs, N. *Adv. Mater.* **1995**, *7*, 842−846.